Energy 114 (2016) 1073–1084

Contents lists available at ScienceDirect

Energy

journal homepage: www.elsevier.com/locate/energy

Net load forecasting for high renewable energy penetration grids

Amanpreet Kaur, Lukas Nonnenmacher, Carlos F.M. Coimbra*

Department of Mechanical and Aerospace Engineering, Jacobs School of Engineering, Center for Energy Research, University of California San Diego, La Jolla, CA 92093, USA

ARTICLE INFO

Article history:
Received 2 January 2015
Received in revised form
16 August 2016
Accepted 19 August 2016

Keywords:
Net load forecasting
High renewable penetration
Microgrids
Solar energy integration

ABSTRACT

We discuss methods for net load forecasting and their significance for operation and management of power grids with high renewable energy penetration. Net load forecasting is an enabling technology for the integration of microgrid fleets with the macrogrid. Net load represents the load that is traded between the grids (microgrid and utility grid). It is important for resource allocation and electricity market participation at the point of common coupling between the interconnected grids. We compare two inherently different approaches: additive and integrated net load forecast models. The proposed methodologies are validated on a microgrid with 33% annual renewable energy (solar) penetration. A heuristics based solar forecasting technique is proposed, achieving skill of 24.20%. The integrated solar and load forecasting model outperforms the additive model by 10.69% and the uncertainty range for the additive model is larger than the integrated model by 2.2%. Thus, for grid applications an integrated forecast model is recommended. We find that the net load forecast errors and the solar forecasting errors are cointegrated with a common stochastic drift. This is useful for future planning and modeling because the solar energy time-series allows to infer important features of the net load time-series, such as expected variability and uncertainty.

1. Introduction

Power grids are undergoing rapid change with increased penetration of variable generation. Specific policies are being developed and implemented to accelerate the penetration of renewable energy technologies associated with wind and solar power, which represent the largest potential for further capacity installation. Based on data from the World Wind Energy Council, 320 GW of wind capacity are currently installed worldwide (about 62 GW in US alone) with a prospective increase up to 2000 GW by 2030. Additionally, world solar energy capacity has increased from 1.28 GW to 138.86 GW over the past decade (2000–2013) [1], with even stronger potential for growth in the next few decades. Due to the stochastic nature of solar and wind power [2], this increasing renewable penetration presents various types of management and operational challenges for the reliable operation of the electric grid on both production and consumption side [3]. On the demand side, it is challenging for grid operators, (e.g. the Independent System Operators (ISOs) or the utilities) to match variable production from intermittent sources with the net load of the customers or the microgrid. This problem intensifies with customers-generators and microgrids with onsite variable generation since the stochasticity in onsite power generation translates into the net load demand from the macro grid. To mitigate these adverse effects, forecasts for expected power generation and net load are needed [4]. There have been significant advancements in the field of load and renewable energy forecasting. Comprehensive reviews are available on load forecasting [5], solar forecasting [6], direct normal irradiance forecasting [7], wind forecasting, and combined wind forecasting methods [8]. However, the integration of these forecasting methods in the operational practices of system operators has gained little attention.

The major contributions of this study are (1) the introduction of the concept of net load forecasting for grids with high renewable energy penetration; (2) the implementation of a solar power prediction algorithm optimized with decision heuristics based on no-exogenous inputs only. This forecast has competitive accuracy in comparison to more complex models and can be used by commercial solar power producers to manage solar power production and plan ahead for the expected ramps in solar energy in data poor environments independently of the integration to a net load forecast; (3) preposition of methods to integrate load and solar

* Corresponding author.
E-mail address: ccoimbra@ucsd.edu (C.F.M. Coimbra).

http://dx.doi.org/10.1016/j.energy.2016.08.067
0360-5442/

Nomenclature

α_s	Solar elevation angle
$\hat{\cdot}$	Forecast of $\cdot$
ϕ	Mapping function
σ	Variance in solar power time-series
τ_D	Hour of the year
τ_Y	Day of the year
$A(q)$	Polynomial with an order n_a
$B(q)$	Polynomial with an order n_b
C	Cost of the error
e	Error
G	Mean solar power
$k_{t,PV}$	Clearness index
L	Length of the values
l_T	Total load
l_{HVAC}	HVAC load
l_{net}	Net load
l_{PV}	Load demand met by PV
M	Maximum solar power
n_k	Input-output delay parameter
n_*	Number of lagged values of the variable *
p_{CS}	Clear sky solar power
p^a_{CS}	Adaptive clear sky solar power
p_{PV}	Solar power
p_S	Stochastic component of solar power
q	Shift operator
S	Maximum deviation from clear sky value
s	Forecast skill
t	Time
u	Input of the model
y	Output of the model

forecasts to create the net load forecast. The net load forecast concept can be adapted for wind forecasting as well; and (4) validating the beneficial characteristics of net load forecasting with data from a microgrid with high penetration of solar power (up to 33% annually).

The paper is structured as follows: Section 2 provides the background of load, demand and production forecasts and introduces the concept of net load forecasting. Section 3 explains the data sets utilized in this study and why a microgrid is used as a testbed. Section 4 contains the proposed methodology. Section 5 discusses the implementation of the model and the results obtained, including an uncertainty for the net load forecast methodology that sheds light on the relationship between the solar and net load forecasting errors. Subsection 5.7 highlights the limitations of the present study. Final conclusions are drawn in Section 6.

2. Background

This section gives a short review of relevant previous work, categorized into solar power generation and load forecasting for power grids. The concept of net load forecasting merging production and load forecasts is presented and its technical and economical benefits for current and future grids are discussed.

2.1. Solar power generation forecasting

Various solar irradiance forecasting techniques using Artificial Neural Networks [9], cloud -tracking [10], sky imagery [11], satellite imagery [12], wavelet model [13], numerical weather prediction [14], harmonic regression [15], cloudiness forecasting [16], etc., have been proposed. Other hybrid methods like combining both satellite and ground imagery [17], classifying sky conditions [18], combining self-organizing maps and Support Vector Regression [19], time-series decompositions and exponential smoothing [20], cuckoo search algorithm [21], etc., have also been proposed and validated. An extensive review on solar forecasting techniques can be found in Ref. [6]. The results from solar forecasting competition were analyzed and it was found that the forecast results can be enhanced by ensemble models and best results were obtained by Gradient Boosting Regression Tree algorithm [22]. While all solar irradiance forecasting methods can be used as an input to forecast solar power output, there have been studies directly forecasting output of solar power plants. Application of regression methods to forecast solar power using weather forecast as an exogenous input has been shown and [23] concluded that the accuracy of solar power forecasts can be increased by 10% by using more accurate weather forecast. Moreover [24], showed that the past values of solar power contribute to the accuracy of forecast model with up to 2 h forecast horizon, thus the use of weather forecasts as an input is recommended for forecast horizons greater than 24 h. A Kalman filter was designed to forecast solar power for cloudy days in Ref. [25]. A methodology to predict solar power forecasting up to 2 days forecast horizon using European Centre for Medium-Range Forecasts (ECMWF) as an input was presented in Ref. [26] and results showed that the proposed methodology adapted to changing weather conditions but overestimated solar production for the snow cover on the modules. Day ahead solar power forecast using Numerical Weather Prediction (NWP) was proposed in Ref. [27] and results show that using forecast the need of operating reserves decrease by 28.6%. A comparison of forecasts for various solar micro-climates considering coastal and continental locations was shown in Ref. [28] and similar forecast skill was achieved irrespective of forecast method.

Furthermore, Artificial Neural Networks (ANNs) based on self-organizing maps using weather forecasts and past power generation as inputs were applied in Ref. [29]. Support Vector Machines (SVM) were used in Ref. [30] for solar power forecasting by classifying the days as clear, cloudy, foggy, and rainy day. In Ref. [31] solar power was forecasted by modeling forecasted GHI where GHI was forecasted using SVM optimized using Genetic Algorithms. Fuzzy theory and ANN based method was proposed in Ref. [32] and the results were validated through computer simulation. Similarly, weather based hybrid method consisting of self-organizing maps and linear vector quantization networks was proposed in Ref. [33] for day ahead hourly solar power prediction. The results showed that hybrid method outperformed simple SVR and traditional ANN methods. All the forecast methods discussed above use exogenous inputs like weather forecasts, sky imagery, etc. Various methods with no exogenous inputs were investigated in Ref. [34]. The study concluded that the ANN based method outperformed all other methods i.e. persistent model, Autoregressive Integrated Moving Average model (ARIMA), and k-Nearest Neighbors (kNNs). Significant improvements can be achieved by optimizing ANN parameters with Genetic Algorithms. NWP-based day-ahead hourly solar power forecast methods were proposed in Ref. [35] with a root mean square error of 10–14% of the plant capacity. All mentioned studies related to solar power forecasting are listed in Table 1.

None of these studies take into account soiling effects, varying

aerosol content in the atmosphere and efficiency degradation of the solar panels over time in forecasting models. The impact of soiling effect is quantified in Ref. [36] and the associated challenges and recommendations for are discussed in Ref. [37]. In Section 4, we propose a solar power output forecast that includes heuristics to account for the changing solar power profiles due to change in seasons, aerosol content in the atmosphere, soiling, etc.

2.2. Load forecasting

Most of the previously proposed techniques for load forecast for power grids are based on artificial intelligence [38], ensemble methods [39], neural network ensembles [40], weather ensembles [41], Support Vector Regression [42], prediction intervals for uncertainty handling [43], socio-economic factors [44] and hybrid models [45], etc. Optimization techniques are applied to select the input variables and hyper-parameters for the forecast model [46]. In many recent studies, application of biologically inspired optimization algorithms like particle swarm optimization [47], firefly algorithm [48], etc are shown for load forecasting problem. The focus of all these studies has been to provide more accurate and reliable load forecasts. The optimal methods for forecasting net load for power grids with high renewable energy penetration have not gained much attention. In Ref. [49] it was shown that onsite solar PV generation impacts the load forecast accuracy when conventional methods are used. An accuracy drop of 3% and 9% for 1-h and 15-min forecast horizon respectively has been reported driven by the variability of the solar resource rather than the solar penetration level. Thus, current industrial forecasting practices have to be updated to accommodate increasing renewable energy penetration.

2.3. Net load forecasting

A study [49] highlights the limitations of current forecasting techniques for systems with onsite solar penetration and quantifies the impact of solar variability on load forecast accuracy [50]. quantified the uncertainty of net load caused by inaccurate wind power output predictions and the impact of increasing solar penetration on net load forecasting capabilities is shown in Ref. [49]. In this study, we pick up the concept of net load uncertainty from Ref. [50] and aggregate solar forecasts to a net load forecast. While this study is based on data from a microgrid with high solar penetration (Section 3.1), the concept of net load forecasting is equally valuable for all kind of power grids with high renewable energy penetration from intermittent generators, explicitly also for interconnected grids with distributed generation from wind and solar energy converters.

A recent study estimated the integration costs for high solar penetration for Arizona State in the United States, which has high solar potential [51]. They concluded that more grid flexibility is needed to lower the integration costs of solar. Photovoltaic generation has the potential to become the main energy source around the world [52]. At present, Germany is the world leader with highest solar penetration, approximately 38 GWp nominal capacity [53]. To manage such a high penetration of renewable energy generation while maintaining secure and stable power grid, needs reliable solar forecasting [53] and as well as net load forecasting.

The need and value of net forecasting around the globe heavily relies on the interconnection regulations and tariffs under which distributed resources or microgrids are tied to a macrogrid or transmission grid. For example, the California Public Utility Commission (CPUC) currently only recognizes three types of tariffs for microgrid interconnection: (1) net-metering, (2) self-generation (impedes export of generated energy and is usually combined with a time-of-use (TOU) tariff when energy has is purchased from the macrogrid) and the (3) wholesale distribution access tariff (WDAT). All of these interconnection options impede to take full advantage of beneficial technical capabilities a microgrid can provide in the energy system since they do not facilitate a bidirectional flow of energy. Many studies highlight the need for better interconnection regulations [54], investments [55] and feed-in tariffs [56], that will enable a better integration of microgrids within the macrogrid, while sharing costs and benefits fairly [57]. Therefore, under current conditions, net load forecasting solely creates economic value by reducing energy purchasing costs for the microgrid operator (optimized load shifting, see Section 3 for details). Under future scenarios, with regulations in place that enable microgrids to

Table 1
Forecast models proposed for solar power forecasting.

Ref.	Inputs	Forecast models	Forecast horizon	Data forecast	Location
[23]	Weather forecast and temperature forecast	Regression method	1 h	Solar power	Expo 205, Aichi Japan
[24]	Weather forecast	Autoregressive and Autoregressive with exogenous input	Up to 36 h	Solar power from 21 PV stationson rooftops	Denmark
[26]	Forecasts from European Center for Medium-Range Forecasts (ECMWF)	Physical model	Up to 2 d	Solar power	Oldenburg, Germany
[29]	Past measurements and meterological forecasts of solar irradiance, relative humidity and temperature	Self-organized map (SOM) and ANN	24 h	Solar power	Huazhong, China
[30]	Temperature	Support Vector Machine	1 day	Solar power	China
[34]	Time-lagged inputs, no-exogenous inputs	Persistent model, Autoregressive Integrated Moving Average model (ARIMA), k-Nearest Neighbor (kNNs), ANN and ANN-GA	1 h and 2 h	Hourly averaged solar power data from 1 MW solar farm	Merced CA, USA
[32]	Weather reported data i.e. clouds, humidity and temperature	Fuzzy theory and Recurrent Neural Networks	24 h	Hourly solar power simulations	–
[33]	Historical PV and weather prediction by Taiwan Central Weather Bureau (TCWB) e.g. temperature, probability of precipitation and solar irradiance	Weather-based hybrid method consisting of Self-Organizing Map (SOM), Learning Vector Quantization (LVQ), Support Vector Regression (SVR) and fuzzy inference method	1-d; every 3-h	Hourly solar power	Taiwan

draw energy from and provide services to the macrogrid, accurate net load prediction becomes important since the load uncertainty at the point of common coupling is an important variable for all interconnection regulations. Market participation and the necessity to minimize the uncertainty introduced by large fleets of interconnected microgrids also requires accurate net load forecasting.

3. Microgrids as testbeds

Various operational decisions of any power grid rely on forecasting. While the findings of this study are generally valid for all power grids with high penetration from intermittent energy sources, the validation of the proposed methods relies on data and findings from microgrids since they provide an excellent testbed for future utility-scale power grids with high renewable generation (e.g. the UC Merced microgrid, see Section 3.1). Experience from existing microgrids and proof-of-concept studies show the need for accurate forecasting of several variables such as load, available demand response capacity, and power-generation for optimized operations [58]. Other theoretical works that involve control and optimization of DERs such solar plus storage [59], electric vehicles [60], etc., can draw benefits from day ahead forecast. Previously, the application of learning techniques for energy management [61], adaptive control [62], and load forecasting for microgrids [63] has been shown. For example, in the case study of Borrego Springs, a microgrid installed and operated as described in Ref. [64], customer load could be curtailed when the forecasting algorithm found benefits for curtailment. Interconnected load forecast is a parameter driving the optimization of microgrid controls and the energy management system [58]. They mention a campus microgrid system with forecasting based optimized resource dispatching, self generation, and grid purchases at Princeton University, New Jersey. Using the load and price forecasts, the mentioned microgrid can buy electricity from the macrogrid based on the hourly wholesale electricity market prices. Optimized purchasing during low energy price times resulted in $2.5 to $3.5 million annual savings. As another example, they mention that the Burrstone Energy Center (3.6 MW_p generation) operates under similar conditions to maximize the economic value of their microgrid. The details about the microgrid used in this study are provided in the next subsection.

3.1. Testbed data

The proposed methodology is applied to forecast solar power and net load demand of University of California, Merced (UCM) situated in San Joaquin valley (see Fig. 1). This community is an ideal test bench to study prospective micro-grids with high solar penetration because it meets 33% of its annual and 3–55% of it's daily power demand by solar energy produced by an onsite 1 MW single axis tracking solar power plant [49]. The Heating Ventilation and Air Conditioning (HVAC) load for the campus is a time-independent load. Unlike conventional buildings where HVAC load is controlled by the users, in this campus HVAC load is segregated from the rest of campus load by means of thermal storage which is completely deterministic load. The chillers to cool down water are turned on/off manually at a fixed time every day. So, we separated deterministic HVAC load from the other loads like lighting and electric motors, etc., because these load change with user's activity every hour and are part of the net load that has to be forecasted. Under current market conditions as discussed above, the advantageous characteristics of net load forecasting as proposed in this study root in the opportunity under tariff option (2) to shift load (e.g. for Heating Ventilation and Air Conditioning (HVAC)) to off-peak hours due to TOU pricing which are lowest at nighttime. Hourly data sets consisting of solar energy production,

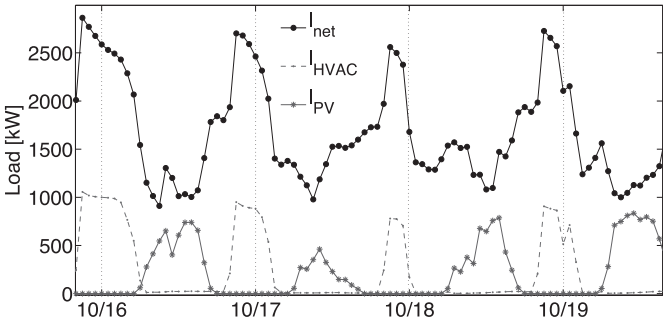

Fig. 1. Block diagram for net load for UC Merced system, l_{net} is the net load demand of the campus from the grid, $l_{HV\,AC}$ is the heating, ventilation and air-conditioning load; and l_{PV} is the solar power output. The intermittence observed in solar power is translated into load demand. Furthermore, at the end of the day the sudden increase in the load demand, also known as duck curve is a major concern for the utilities.

HVAC load and load demand from the grid are utilized for this study.

The data was time synchronized and pre-processed to remove outliers. Data for the year 2010 consisting of 5546 data-points are considered as a training set and data for the year 2011 with 7548 data-points are considered as a testing set. Using data sets for the whole year as training and test sets encompass all seasonal variations for the given location.

4. Proposed methodology

The net load from the grid l_{net} for any given time t can be expressed as,

$$l_{net}(t) = l_T(t) - l_{PV}(t), \tag{1}$$

where $l_T(t)$ is the total UCM load, l_{PV} is the load demand met by an onsite solar generation i.e., l_{PV} is equal to the onsite solar power generation p_{PV}. Since, thermal storage plant for HVAC load is operated manually, it is assumed to be a deterministic load for this study 3.1 and is not included in Equation (1). Thus, total load demand from the grid $l_T(t)$ can be decomposed into deterministic and stochastic part $l_s(t)$,

$$l_T(t) = l_s(t) + l_{HV\,AC}(t). \tag{2}$$

Comparing Equations (1) and (2), forecasting net load simplifies to forecasting stochastic part which is equivalent to,

$$\widehat{l}_{net}(t) = \widehat{l}_s(t) + l_{HV\,AC}(t) - \widehat{l}_{PV}(t), \tag{3}$$

where $\widehat{l}_{net}$ represents forecast for l_{net}, and similarly $\widehat{l}_s$ and $\widehat{l}_{PV}$ are forecasts for l_s and l_{PV} . The algorithms to forecast solar power and net load are discussed in the next subsection.

4.1. Solar power forecast

Solar power $p_{PV}(t)$ at any time t can be considered as a sum of deterministic clear sky solar power $p_{CS}(t)$ and stochastic component i.e.,

$$p_s(t) = p_{PV}(t) - p_{CS}(t). \tag{4}$$

The clear sky solar power $p_{CS}(t)$ is a function of day of the year, latitude, longitude of the location which are all deterministic factors. But it is also affected by various daily and seasonal processes due to changing linke-turbidity factor, soiling and temporal degradation of solar panel efficiency [36]. To account for these

factors, adaptive clear sky solar power identification to update daily clear solar power is presented. To correct for overcast conditions, morning and evening time values heuristics are proposed.

4.1.1. Clear sky solar power identification

Clear sky solar irradiance is deterministic and can be modeled as a function of hour of the day τ_D, day of the year τ_Y, latitude and longitude of the location. But in case of clear sky solar power p_{CS} along with the deterministic part, p_{CS} is continuously affected by the seasonal change, aerosol content in the atmosphere, dust accumulating on the solar panel, temperature dependent efficiency of solar panel, solar panel degradation over the time and so on [37]. This continuous change adds to the forecast errors. These factors can be accounted empirically based on most recent available information about the system. Thus, adaptive clear model p^a_{CS} that takes into account the recent changes in clear sky solar power is proposed here. This step ensures an accurate separation of deterministic and random components of the solar power after deterending. Solar power based clearness index, $k_{t,PV} = \frac{p_{PV}}{p^a_{CS}}$ is defined and the value of $k_{t,PV}$ ranges between 0 and 1. At the end of the day, five clear sky criteria introduced by Ref. [65] are applied to check if the clear sky model should be updated or not. The five criteria are briefly defined below.

1. Mean solar power value during the time period,

$$\overline{G} = \frac{1}{N}\sum_{t=1}^{N} p_{PV}(t). \tag{5}$$

2. Maximum irradiance value in the time-series,

$$M = \max\{p_{PV}(t)\} \quad \forall t \in \{1, 2, \cdots, N\}. \tag{6}$$

3. Length of the line formed by p_{PV} values in the time-series,

$$L = \sum_{t=1}^{N} \sqrt{(p_{PV}(t+\Delta t) - p_{PV}(t))^2 + (\Delta t)^2}. \tag{7}$$

4. Maximum deviation from the clear sky slope,

$$S = \max\{|s(t) - s_c(t)|\} \quad \forall t \in \{1, 2, \cdots, N\}, \tag{8}$$

where,

$$s_c(t) = p_{CS}(t+\Delta t) - p_{CS}(t). \tag{9}$$

5 Variance in the time-series,

$$\sigma = \frac{\sqrt{\frac{1}{N-1}\sum_{t=1}^{N-1}(s(t) - \overline{s})^2}}{\frac{1}{N}\sum_{t=1}^{N} p_{PV}(t)}, \tag{10}$$

where

$$s(t) = p_{PV}(t+\Delta t) - p_{PV}(t) \quad \forall t \in \{1, 2, \cdots, N\}, \tag{11}$$

and

$$\overline{s} = \frac{1}{N-1}\sum_{t=1}^{N-1} s(t). \tag{12}$$

To make the identification criteria more robust, after checking for threshold, the measured values of the clearness index are also considered. If the clearness index values for the day time are greater than 0.90 then the day is considered as clear day and the clear sky solar power model is updated. Here are the summarized steps:

- **Inputs:** Hourly values of solar power p_{PV};
- **Output:** Identified clear sky solar power p^a_{CS};
- initialize p^a_{CS};
- **For** all unique days **do:**
  - compute G, M, L, S, σ and k_t at the end of the day;
  - **If** $G < G_t$ & $M < M_t$ & $L < L_t$ & $S < S_t$ & $\sigma < \sigma_t$: update clear sky model, p^a_{CS};
  - **Else if** $k_{t,PV} > 0.90$: update clear sky model, p^a_{CS};

4.1.2. Heuristics

Solar power forecast is produced using a base model. In this study we consider Support Vector Regression model as a base model. The forecast model produces de-trended solar output and the adaptive clear sky solar power is added at the end i.e.,

$$\widehat{p}_{PV}(t) = \widehat{p}_S(t) + p^a_{CS}(t). \tag{13}$$

Adding clear solar power always tends to overestimate solar irradiance for overcast conditions (see Fig. 3 for early morning period on 03/02/2011 and 03/06/2011). To correct for this issue, heuristics based on persistence assumption are applied for solar elevation angle $\alpha_s > -2$. It assumes that for overcast conditions i.e. $kt_{pv}(t-1) < 0.30$, the forecast will be a sum of past values and current weather conditions times the base model forecast value. Below are the summarized steps:

- **Input**: $\widehat{p}_{PV}, k_{t,PV}, \alpha_s$;
- **Output:** Updated solar forecast, $\widehat{p}^h_{PV}$;
- **While** $\alpha_s > -2$ **do**:
  - **If** $kt_{PV}(t-1) < 0.30$: $\widehat{p}^h_{PV}(t, \alpha_s) = \widehat{p}_{PV} k_{t,PV}(t-1) + p_{pv}(t-1)$;
  - **Else**: $\widehat{p}^h_{PV}(t, \alpha_s) = \widehat{p}_{PV}$;

The base model used in this paper depends on the past lagged values. Since, at the beginning of the day (sunrise) the inputs are past night time values which are equal to zero, there is a discontinuity in data as night values do not give any useful information about the first hour of the sun rise. Most of the solar irradiance forecast studies ignore the solar irradiance/power values for solar zenith angle less than 5 or 15° [11] because the values of solar irradiance/solar power are negligible as compared to rest of the day time values. But in the case of net load forecasting, a continuous forecast of solar power for all the hours is needed. Therefore, we assume the first morning value to be the clear sky solar value. Similarly, the last value before the sunset is so small that the affect of atmospheric condition is negligible and hence, it is assumed to be equal to the clear sky value.

4.2. Net load forecast

We compare two approaches to perform net load forecasting: additive and integrated model. In case of additive model, the net load forecast is performed as,

$$\widehat{l}_{net}(t) = \widehat{l}_T(t) - \widehat{l}_{PV}(t). \tag{14}$$

Whereas in the integrated model, solar power forecast is used as an input to net load forecasting model. Deterministic l_{HVAC} is added

to the net load forecast at the end. Both the methods are tested by implemented time-series and machine learning based forecast models i.e. Autoregressive model and Support Vector Regression model.

4.2.1. Autoregressive model (AR)

AR model is a linear time-series regression model. Using this model, the output can be expressed as linear combination of past outputs/measured values i.e.,

$$A(q)y(t) = e(t) \tag{15}$$

where q^N is shift operator i.e., $q^{\pm N} = l_{net}(t \pm N)$, $A(q)$ represents the combination of past values of output using coefficients, $a_1, a_2, \cdots, a_{na}$ and $A(q) = 1 + a_1 q^{-1} + \cdots + a_{na} q^{-na}$. The part of the time-series not modeled is represented as $e(t)$. For more details refer to [66].

4.2.2. Autoregressive model with exogenous input (ARX)

ARX model is an extension of AR model with an addition of external inputs. In this study the external input, $u(t)$ consists of solar power forecast values and past measured solar power. Mathematically, it can represented as,

$$A(q)y(t) = B(q)u(t - n_k)(t) + e(t) \tag{16}$$

where $B(q) = b_1 + \cdots + b_{nb} q^{-nb+1}$, n_k is time delay parameter, it is equal to zero for solar power forecast and 1 for the past values of the measured solar power.

4.2.3. Support Vector Regression (SVR)

Support Vector Regression technique is based on supervised machine learning algorithm [67]. A detailed tutorial on SVR is presented in Ref. [68]. It has been widely applied for forecasting various kind of time-series such as finance [69], load [70], stock market [71], etc. Given the training data $\{(u_1, y_1), \cdots, (u_l, y_l)\} \subset U \times \mathbb{R}$ where U denotes the space of input pattern. The goal is to find a function $f(u)$ that has at-most ε deviation from the actually obtained targets y_i,

$$f(u) = \langle w, u \rangle + b \quad \text{with} \quad w \in U, b \in \mathbb{R}. \tag{17}$$

Support Vector regression solves the following optimization problem,

$$\min_x \quad \frac{1}{2} w^T w + C \sum_{0 < i < m} (\xi_i + \xi_i^*), \text{subject to} \quad y_i - \left(w^T \phi(u_i) + b\right) \leq \varepsilon + \xi^*, \; \left(w^T \phi(u_i) + b\right) - y_{ti} \leq \varepsilon + \xi^*, \; \xi_i, \xi_i^* \geq 0, i = 1, \cdots, l, \tag{18}$$

where $\phi(u)$ is maps u_i to a higher dimensional space using a kernel function and the training errors are subject to ε-insensitive tube $y_i - (w^T \phi(u_i) + b) \leq \varepsilon$. Cost of the error, C, width of the tube and the mapping function ϕ controls the regression quality.

For this study, time series formulation is applied i.e.,

$$y_t = f(u(t)). \tag{19}$$

The details about $y(t)$ and $u(t)$ are given in Table 3, where $n*$ represents the number of lagged values of the variable $*$. Because of the use of external input into the SVR model for integrated net load forecasting model, we term it as SVRX to avoid ambiguity.

5. Model implementation and discussion of results

For the clear sky identification model, the thresholds for G_{th}, L_{th}, M_{th}, S_{th} and σ_{th} were obtained using the training set given Table 2. These thresholds can be updated for other sampling frequencies for both solar power and solar irradiance.

For the forecast model, LIBSVM: A Library for Support Vector Machines [72] was used. Parameter were selected using grid search by v-fold cross validation technique. The SVR optimization problem was simplified to finding C and γ values as discussed in Ref. [42]. The solar power data was scaled linearly in the range of [0.1 1]. For the SVR model, a radial basis kernel function was used. To select the number of lagged inputs Rissanen's Minimum Description Length (MDL) criterion was applied. The model with derived parameters was trained using the whole training set and was validated using the testset.

For integrated net load forecasting, the solar power forecast produced using the above algorithm was used as one of the input parameter for the training model. Also, note that there were some days in the training and test set when net load was negative due to excessive solar generation. To account for negative values, the net load was scaled linearly between [−1 1].

Various statistical metrics are applied to quantify the results. The forecast results are reported in terms of Mean Absolute Percentage Error (MAPE), Mean Bias Error (MBE), Mean Absolute Error (MAE), Root Mean Square Error (RMSE) and coefficient of determination (R^2). MAPE is very sensitive to high magnitude errors when actual value is very small. In this work, the forecast and actual value are removed in computing MAPE when actual value for net load or solar power are less than 0.05 kW.

Furthermore, Persistence model, is implemented based on the assumption of that current conditions are likely to persist in future,

$$\hat{y}(t) = y(t - 1). \tag{20}$$

An extension of persistence model is Smart Persistence (SP) model that takes into account for deterministic information available about the system. For this model, the forecast is sum of present stochastic component of solar power that is assumed to persist in future and deterministic future clear sky solar power value i.e.,

$$\hat{p}_{pv}(t) = p_s(t - 1) + p_{CS}(t). \tag{21}$$

SP is used as a reference model to validate the goodness of solar forecast models. The performance of the proposed model is compared to that of a SP model in terms of forecast skill (s) [73], which is defined as,

$$s = 1 - \frac{RMSE_{model}}{RMSE_{SP}}. \tag{22}$$

5.1. Clear sky identification

The clear sky identification algorithm was applied to identify the clear days and update the clear sky solar irradiance model, p_{CS}^a. The results for the identification algorithm are given on Table 4. For the training set, there were total of 228 days, out of which 109 were clear days. The algorithm identified a total of 115 clear days, out of

Table 2
Thresholds for clear sky solar power identification.

G_t	M_t	L_t	S_t	σ_t	k_t	N	Δt
150	220	220	120	0.12	0.90	3	1 h

Table 3
Output and input variables for the SVR model.

Forecast model	$y(t)$	$u(t)$
Solar power	$p_s(t)$	$p_s(t-1), p_s(t-2), \cdots, p_s(t-n_{p_s})$
Additive model	$l_t(t)$	$l_t(t-1), l_t(t-2), \cdots, l_t(t-n_{l_t})$
Integrated	$l_{net}(t)$	$l_{net}(t-1), l_t(t-2), \cdots, l_t(t-n_{l_{net}}), \widehat{p}_s(t), \cdots,$ $\widehat{p}_s(t-n'_{p_s}), p_s(t-1), p_s(t-2), \cdots, p_s(t-n''_{p_s})$

which 101 days were truly clear days, whereas 14 days were falsely identified as clear and 8 days were missed. Given that the accuracy of the algorithm is defined as percentage of actual clear in total number of clear days identified, for the training set the accuracy is 87.82% and for the testing set it is 84.12%. Incorrect identification happens for the days with very small ramps that do not exceed the threshold range as shown in Fig. 2. The disadvantage of identifying incorrect days is that unnecessary ramps in the solar power are introduced which affect the accuracy of the forecast. This does not happen very often as the model auto-corrects itself (e.g. in Fig. 2 it can be observed that 07-11-2011 was identified incorrectly as clear day and a false ramp was introduced for 07-12-2011, but this was autocorrected by 07-13-2011). The errors introduced by identifying incorrect days can be ignored because they are small in magnitude as compared to the improvements achieved in forecasting as discussed in the next section.

5.2. Solar power forecast

An hour ahead solar forecast was implemented using SP and SVR as base model. Firstly, the forecast models based on clear sky solar power using τ_D and τ_Y were implemented. In the next step, the basic clear sky model was replaced with the adaptive clear sky model as explained in Section 4.1.1. The improved models were termed as SP_α and SVR_α. Finally, heuristics as proposed in Section 4.1.2 were applied to the models and termed as $SP_{\alpha,h}$ and $SVR_{\alpha,h}$. All the results and corresponding improvements are listed in Table 5. MAPE significantly reduces for models with adaptive clear sky model and heuristics. MBE gives the information about the bias in the error. For all the results reported in this study MBE error is negative which suggests that the forecast models always overestimate the power forecast. Furthermore, the MAE gives information about the net error in forecast which is about 44.33 kW i.e., 4.4% of the maximum rating capacity of the power plant. The deviation in forecast values as compared to the actual values is given by the RMSE. It is a scale dependent measure and gives the information in terms of standard deviation w.r.t. the mean.

An adaptive clear sky model ensures that daily variability is taken into account. Thus, by its application the RMSE reduces from 113.78 kW to 103.08 kW for SP and 109.04 kW−100.80 kW for SVR which is an improvement of 9.40% for SP model and 7.56% for SVR model. Since, the night values give no information about the overcast in the morning, major error was observed in the morning. To correct for such error heuristics were applied and an improvement of 14.57% for SP and 14.44% for SVR model was observed. The statistical metrics show the improvements achieved by using the adaptive clear sky model and then further possible improvements by applying heuristics. Since all these results are achieved without using any exogenous input, the proposed technique can serve as reference to compare the forecast models with exogenous inputs.

Table 4
Clear sky identification results.

Data set	Total days	Actual clear days	Clear days identified			
			Total	True	False	Missed
Tset	228	109	115	101	14	8
Vset	300	119	126	116	10	3

5.3. Net load forecast

The net load forecast was implemented using: 1) additive model where solar and load forecast were produced individually and then combined at the end and 2) integrated model where the solar power forecast was used as input into the load forecast model. The forecast error statistics for the additive model and the proposed integrated net load forecasting model are listed in Table 6. The stationarity of errors is shown in Fig. 5 as there is no correlation over the hourly time lags. This validates the model identification because all the information in the time-series has been captured.

The results show that the integrated model outperforms the additive models marginally in terms of all error metrics (see Fig. 6). In case of Autoregressive model, integrated ARX model performs 9.35% better than the additive AR model and SVRX performs 10.69% better than the SVR model in terms of RMSE. Fig. 6 shows that the spread of additive model forecast errors is more than the integrated model. This validates the lower RMSE for integrated model as compared to the additive model. Thus, integrated model should be preferred for the grid applications.

If compared in terms of MAPE and MBE, time-series based AR model always perform better than the SVR model. Whereas in case of MAE and RMSE, SVR model outperforms the AR model for both additive and integrated case. Sample results are shown in Fig. 4. For overcast days (11-07-2011 (early morning) and 11-11-2011), it can be observed that the solar power model tends to over-predict the initial value. This is due to addition of clear sky solar power and discontinuity in solar data at early morning hours. The forecast error uncertainty is quantified in the next section.

5.4. Assessment of forecast uncertainty

The forecast uncertainty can be quantified using the 95% confidence interval. Using the inverse Cumulative Distribution Frequency, the 95% confidence interval corresponds to 2.5 to 97.5 percentile of the distribution reflecting the uncertainty. Freedman-Diaconis rule is applied to define the number of bins for the data sets and the results are shown in Fig. 7. Based on the previous discussions and comparison, it is expected that the uncertainty range for the additive model will be larger than the integrated model. The results show that the uncertainty range for additive model is between −218 kW and 241 kW and for the integrated model the range is from −214.5 kW to 198.6 kW. The maximum value of the net load during the daytime is 2.07 MW. Taking the absolute values, the uncertainty increases by 46 kW for the additive model as compared to the integrated model which is equivalent to 2.2% of maximum net load. Furthermore, for the solar forecasting errors, the uncertainty range is between −213 kW and 195 kW. This is very close to the range of integrated model and it could be a good approximation for the net load forecast errors. The relationship between the solar and net load forecast errors is established in the next section.

5.5. Solar and net load forecast errors

For future planning and modeling for the grids with expected high solar penetration, it is important to quantify the relationship between the solar and net load forecast errors. However, as shown in Fig. 5 and discussed previously, both solar and net load errors are stationary and yet Fig. 6 shows that the solar forecast and net load

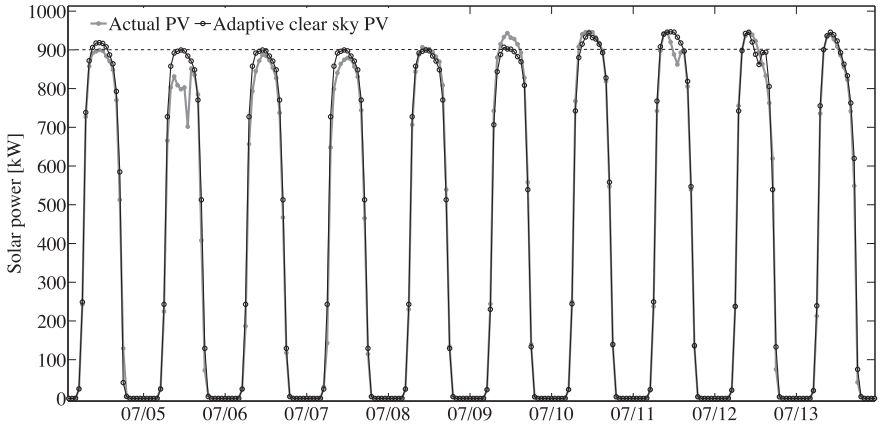

Fig. 2. Time series for the solar power generated for the 10 consecutive days from the year 2011. Dashed line indicates a reference level at 900 kW and it can be observed that after 07/08 the maximum solar power exceeds the reference level. Adaptive clear sky model takes into account these kind of changes and updates the clear sky model. Even though 07/11 is a cloudy day, it was identified as a clear day. However, the adaptive clear sky identification algorithm autocorrects itself and it was updated by another clear sky model for 07/13.

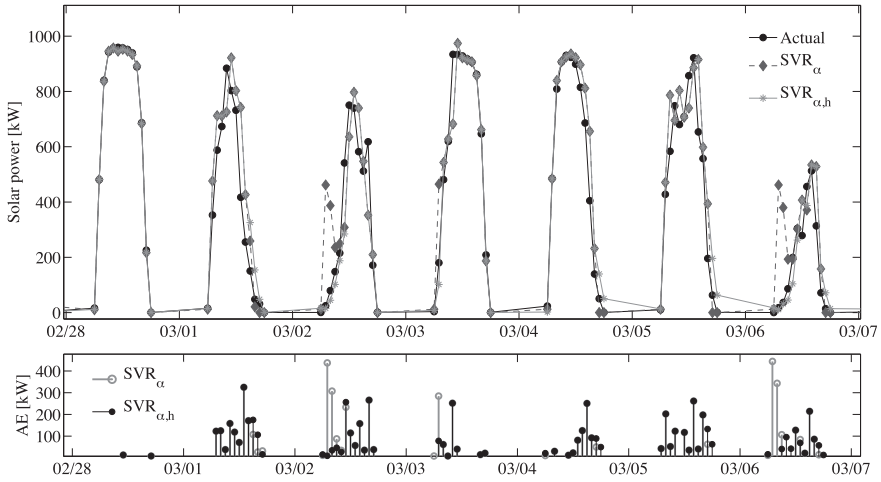

Fig. 3. Time series for the actual solar power and forecast for 1-h forecast horizon (top) and absolute error, AE (bottom) with night values removed. Here we can compare the results from SVR$_\alpha$ and SVR$_{\alpha,h}$ model. For the overcast period, SVR$_{\alpha,h}$ is able to correct for the over-predicted solar power by SVR$_\alpha$. For a cloudy day with ramps (03/01/2011 and 03/05/2011), both the models have similar errors. The SVR$_{\alpha,h}$ model works better than SVR$_\alpha$ model in detecting overcast conditions and correcting for errors in the morning time (03/02/2011 and 03/06/2011).

Table 5
Statistical error metrics for hour-ahead solar power forecast (for the period ranging from 01-01-2011 to 12-31-2011).

Model	MAPE (%)	MBE (kW)	MAE (kW)	RMSE (kW)	R^2	Skill s(%)
Using clear sky model based on τ_D and τ_Y						
SP	349.08	−9.15	74.44	113.78	0.90	0
SVR	291.18	−12.92	72.08	109.04	0.91	4.17
Using adaptive clear sky model						
SP$_\alpha$	144.78	−9.30	52.29	103.08	0.92	9.40
SVR$_\alpha$	113.47	−16.17	52.19	100.80	0.92	11.41
Applying heuristics						
SP$_{\alpha,h}$	101.36	−2.37	44.76	88.06	0.94	22.61
SVR$_{\alpha,h}$	101.12	−5.82	44.33	86.24	0.94	24.20

Table 6
Statistical error metrics for UCM load demand forecast (for the period ranging from 01-01-2011 to 12-31-2011).

Model	MAPE (%)	MBE (kW)	MAE (kW)	RMSE (kW)	R^2
PV forecast including night time values					
SVR$_{\alpha,h}$	141.07	−2.20	25.59	65.06	0.97
Persistence model for net load forecast					
Persistence	10.93	0.07	152.77	240.92	0.83
Additive model: Model − SVR$_{\alpha,h}$					
AR	13.98	4.58	64.99	93.83	0.97
SVR	30.47	3.76	63.88	92.48	0.97
Integrated solar power (SVR$_{\alpha,h}$) and net load forecast					
ARX	4.60	4.60	57.75	85.06	0.98
SVRX	5.47	5.47	54.74	82.59	0.98

forecast errors are inversely proportional to each other. To test for hidden correlation between these time-series, cointegration test is applied and discussed below.

5.6. Cointegration of solar and net load forecast errors

The concept of spurious regression [74] and cointegration was first introduced by Ref. [75]. It is used to define statistical properties of the time-series. Time-series are cointegrated if they share a common stochastic drift. Two random variables are cointegerated if one random variable, $x(t)$ can be expressed linearly in terms of second random variable, $w(t)$ using some coefficient β i.e.,

$$x(t) - \beta w(t) = e(t) \tag{23}$$

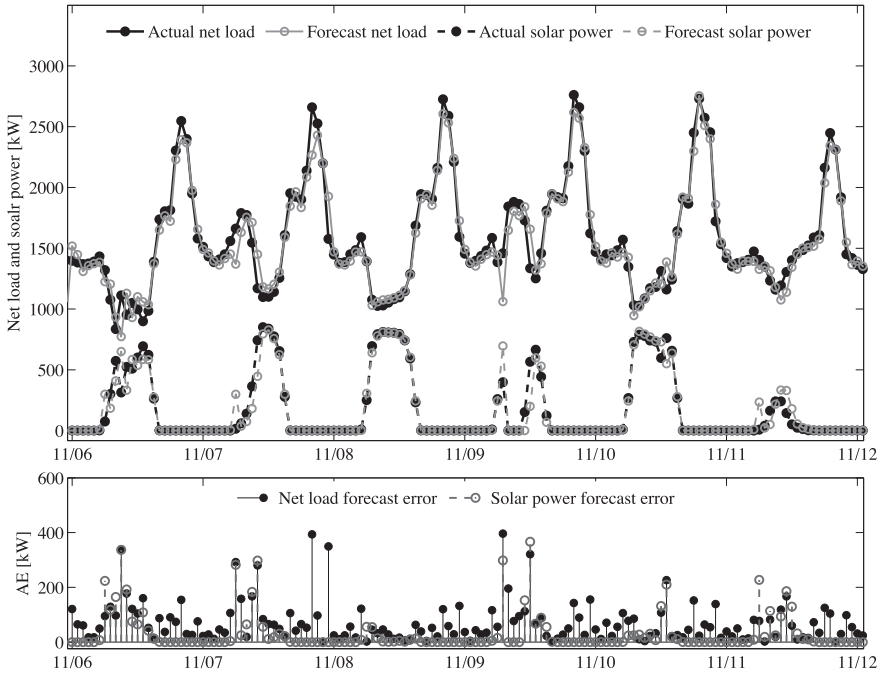

Fig. 4. Time series for the net load and solar power forecast for six consecutive days (11/06/2011 to 11/12/2011) from the testset. The absolute error (AE) in the forecasts is shown in the figure below. It can noticed that the solar forecast error directly influences the net load forecast. Solar power is always over-predicted for the days with overcast conditions (11/07/2011 and 11/11/2011). Heuristics are introduced to correct for these errors. Magnitude of net load forecast error is less for clear (11/08/2011) and overcast days (11/11/2011) as compared to the cloudy days.

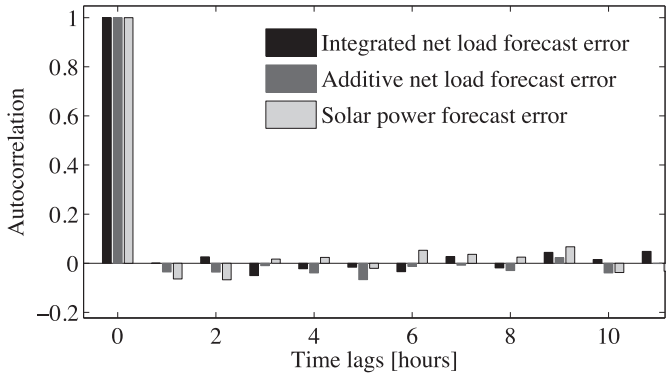

Fig. 5. Error correlation for net load forecast models. After zero lag, there is no correlation in forecast errors. This establishes that all the information in time-series have been captured by the forecast model and the forecast residues are randomly distributed.

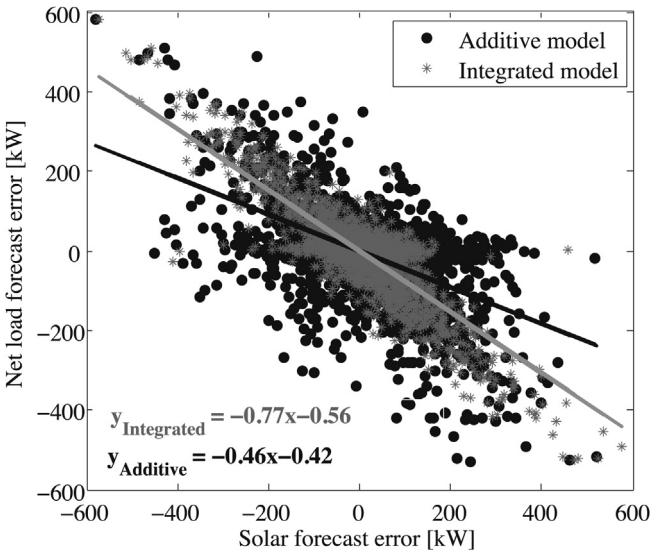

Fig. 6. Comparison of net load forecast errors for both additive and integrated models with respect to the solar forecast errors from $SVR_{\alpha,h}$ model during daytime. Night time values have been removed for this plot and analysis. The net load forecast errors are inversely proportional to solar forecast errors. The linear fit predicts 98% variance of the integrated forecast errors and 83.59% variance of the additive model forecast errors.

such that the residue, $e(t)$ after fitting is stationary [76]. $e(t)$ is also known as cointegrating relation. Here, we apply this concept on net load and solar forecast errors. This step ensures that the correlation between two random variables is not spurious and furthermore, error-correction models can be applied for modeling such pair of time-series.

The Engle-Granger cointegration test was applied with the null hypothesis that the net load and solar forecast error time-series are not cointegrated. Results (see Fig. 8) were against the hypothesis with stationary cointegrating relation. Hence, net load and solar forecast errors are co-integrated time-series. This validates the correlation presented in Fig. 6. Therefore, the relationship between net load and solar forecast errors can be represented as

$$\widehat{e}(t)_{integrated} = -0.77e(t)_{solar} - 0.56, \tag{24}$$

and

$$\widehat{e}(t)_{additive} = -0.46e(t)_{solar} - 0.46. \tag{25}$$

Using the equations presented above, 98% of the variance of

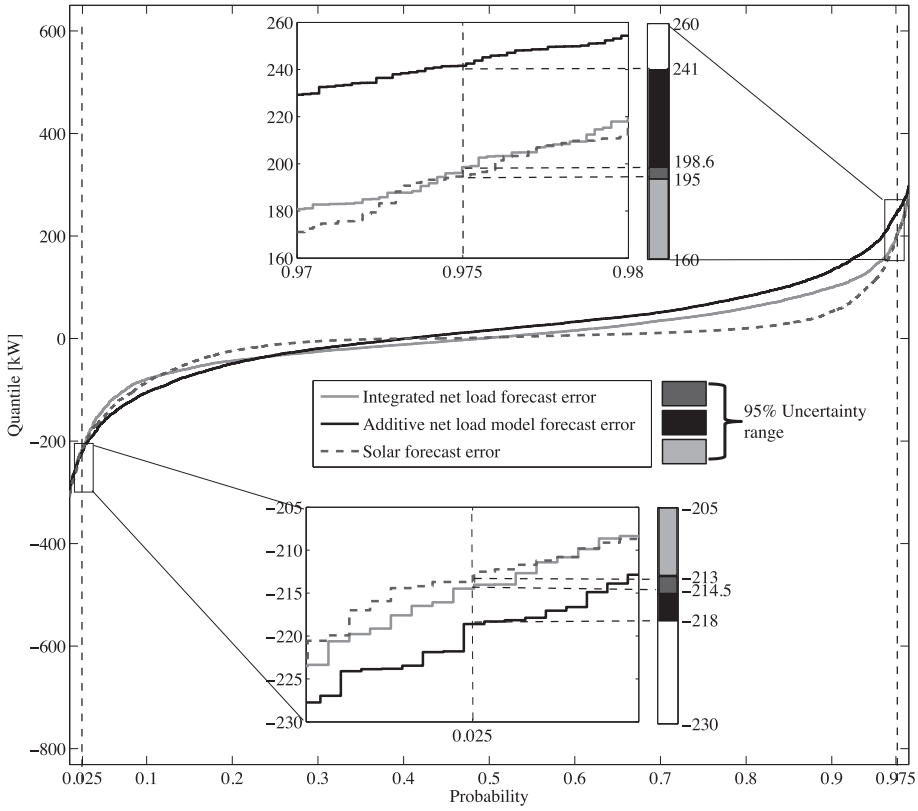

Fig. 7. Net load and solar forecast uncertainty assessment by applying inverse CDF during daytime. The quantile represents the forecast errors in kW. The upper and lower inset plots show upper and lower bound for the 95% confidence interval for the forecast errors. The 95% confidence interval for the additive net load forecast model ranges between −218 kW and 241 kW (black), for the integrated model this range is −214.5 kW to 198.6 kW (dark grey) and for the solar forecast errors the range is −213 kW to 195 kW (light grey). Thus, the uncertainty range decreased by 46 kW by using the integrated model.

integrated net load forecast errors can be predicted using solar forecast errors whereas only 83.59% of the variance of additive net load forecast errors can be predicted using solar forecast errors.

5.7. Limitations of the present study

In principle, the results obtained in this work could be extended to residential microgrids as well with centralized community solar/wind farm or distributed solar rooftop systems. The availability of reliable, real-time forecasts for total solar or wind generation at the local level is required to extend the proposed methodology to these situations. This is a major limitation of this model because short-term forecasts for intermittent resources like solar/wind are not readily available at the local level. Remote sensing-based forecasts, which can be readily implemented to any region, lack both the spatial resolution and the ability to produce high-resolution intra-half hour forecasts. In the case of wind generation, numerical weather prediction models can be used to predict general wind trends, but these models also lack the temporal resolution to generate accurate short-term (less than 15 min) forecasts, even at the highest resolutions and lowest computational latencies currently available. In this study, we discuss forecasts for centralized generation only. For distributed systems, similar ideas could be extended when forecasting the net load at the substation/feeder/microgrid level. But in these situations, the major challenge in extending this model would be to generate forecasts for all the installed systems under a substation/feeder/microgrid domain area, i.e., the problem of resolving both spatially and temporally a diverse distribution of feeders. For systems with mixed energy generation profile, combined forecasts for all the energy generation resources are needed to integrate into net load forecasting model. Nonetheless, the present study suggests the possibility of developing scale-specific models that could overcome the current model restrictions for other applications and scales.

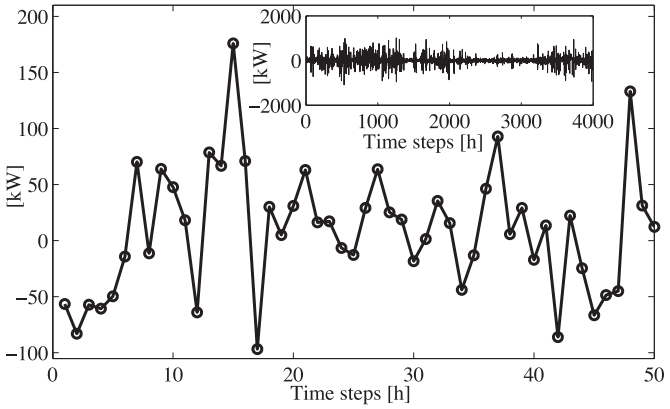

Fig. 8. Cointegrating relation between the hourly integrated net load and solar forecast errors during the daytime for the first consecutive 50 h. Inset plot shows the cointegrating relation for the whole time-series. The combination is indeed stationary, which validates the cointegration of the time-series and negates the possibility of spurious regression.

6. Conclusions

This study introduces the concept of micro-to-macro grid net load forecasting and discusses its technical and economical benefits for interconnected grids. An implementation of the proposed forecasting methodology is presented for a commercial microgrid with high solar penetration. Two different net load forecasting approaches using load and a solar power output forecasts are implemented and evaluated: integrated and additive.

To predict solar power a heuristics based approach with no exogenous input is presented. The proposed approach takes changing atmospheric clearness, panel soiling and efficiency degradation of PV panels into account using adaptive clear sky model and heuristics. The accuracy of clear sky solar identification was found to be 84.12% for the region and period under study. Adaptive clear sky solar power showed an improvement of 9.4% and the heuristics proposed in this study further showed an improvement of 22.61% over the smart persistence model. For the SVR model, the improvement was 11.41% for the adaptive clear sky model and 24.20% after the heuristics were applied. Thus, the adaptive clear sky model and the heuristics proposed in this study should be applicable to other solar forecasting algorithms in order to improve forecast accuracy.

As stated above, the solar power forecast is applied for two different net load forecasting approaches. The integrated solar and load forecast model outperformed the additive model by 10.69% in terms of Root Mean Square Error (RMSE) for the SVR and SVRX models. The forecasting model implemented in this study tends to over-predict solar power for overcast periods in the early morning time and hence, under-predict net load for the corresponding time. Over the day, frequent forecast errors were observed during cloudy periods as compared to overcast periods which is in agreement with the findings in Ref. [49].

Uncertainty ranges for the net load and solar power forecast errors were analyzed. The 95% confidence interval for the additive model is larger than the integrated forecast model by 2.2% of the maximum net load demand. The 95% confidence interval of solar forecast can be used as an approximation for the expected accuracy of the net load forecasts. There is high correlation between the net load forecast errors and solar forecast errors. To validate the correlation between the solar and net load error time-series, the Engle-Granger cointegration test was applied. The two stationary time-series are indeed cointegrated and hence, share the common stochastic drift. Using solar forecast errors, 98% variance of net load forecast errors can be predicted. Thus, solar power time-series is sufficient to provide necessary information to characterize the expected variance and uncertainty in the net load time-series.

In summary, the present work suggests that for microgrid applications (and to lesser extent for interconnected utility grids), the use of an integrated net load forecasting model leads to a reduction in the uncertainty at the point of coupling at the interconnection. An analogous net load forecasting model can also be adapted for grids with high penetration of other renewable resources by, for example, using wind forecast models as an input (within the restrictions highlighted in Subsection 5.7). The proposed concept has the potential to enable grid operators to efficiently manage grids with high intermittent renewable energy penetration in order to participate in electricity market for economic benefits.

Acknowledgements

Partial funding for this research was provided by the California Public Utilities Commission under the California Solar Initiative Program Grant No. 4 (CSI 4). Partial funding from San Diego Gas & Electric is also gratefully acknowledged.

References

[1] EPIA - European Photovoltaic Industry Association. Global market outlook for photovoltaics 2014–2018. 2014.
[2] Nonnenmacher L, Kaur A, Coimbra CFM. Verification of the suny direct normal irradiance model with ground measurements. Sol Energy 2014;99(0):246–58.
[3] Zagouras A, Inman RH, Coimbra CFM. On the determination of coherent solar microclimates for utility planning and operations. Sol Energy 2014;102(0):173–88.
[4] Hahn H, Meyer-Nieberg S, Pickl S. Electric load forecasting methods: tools for decision making. Eur J Oper Res 2009;199(3):902–7.
[5] Suganthi L, Samuel AA. Energy models for demand forecasting a review. Renew Sustain Energy Rev 2012;16(2):1223–40.
[6] Inman RH, Pedro HT, Coimbra CFM. Solar forecasting methods for renewable energy integration. Prog Energy Combust Sci 2013;39(6):535–76.
[7] Law EW, Prasad AA, Kay M, Taylor RA. Direct normal irradiance forecasting and its application to concentrated solar thermal output forecasting a review. Sol Energy 2014;108(0):287–307.
[8] Tascikaraoglu A, Uzunoglu M. A review of combined approaches for prediction of short-term wind speed and power. Renew Sustain Energy Rev 2014;34(0):243–54.
[9] Marquez R, Gueorguiev VG, Coimbra CFM. Forecasting of global horizontal irradiance using sky cover indices. J Sol Energy Eng 2012;135(1):011017.
[10] Marquez R, Coimbra CFM. Intra-hour DNI forecasting based on cloud tracking image analysis. Sol Energy 2013;91:327–36.
[11] Chu Y, Pedro HTC, Coimbra CFM. Hybrid intra-hour {DNI} forecasts with sky image processing enhanced by stochastic learning. Sol Energy Part C 2013;98(0):592–603.
[12] Nonnenmacher L, Coimbra CFM. Streamline-based method for intra-day solar forecasting through remote sensing. Sol Energy 2014;108(0):447–59.
[13] Mellit A, Benghanem M, Kalogirou S. An adaptive wavelet-network model for forecasting daily total solar-radiation. Appl Energy 2006;83(7):705–22.
[14] Amrouche B, Pivert XL. Artificial neural network based daily local forecasting for global solar radiation. Appl Energy 2014;130(0):333–41.
[15] Trapero JR, Kourentzes N, Martin A. Short-term solar irradiation forecasting based on dynamic harmonic regression. Energy 2015;84(0):289–95.
[16] Alonso J, Batlles F. Short and medium-term cloudiness forecasting using remote sensing techniques and sky camera imagery. Energy 2014;73(0):890–7.
[17] Marquez R, Pedro HTC, Coimbra CFM. Hybrid solar forecasting method uses satellite imaging and ground telemetry as inputs to {ANNs}. Sol Energy 2013;92(0):176–88.
[18] Alonso-Montesinos J, Batlles F. Solar radiation forecasting in the short- and medium-term under all sky conditions. Energy 2015;83:387–93.
[19] Dong Z, Yang D, Reindl T, Walsh WM. A novel hybrid approach based on self-organizing maps, support vector regression and particle swarm optimization to forecast solar irradiance. Energy 2015;82(0):570–7.
[20] Yang D, Sharma V, Ye Z, Lim LI, Zhao L, Aryaputera AW. Forecasting of global horizontal irradiance by exponential smoothing, using decompositions. Energy 2015;81(0):111–9.
[21] Wang J, Jiang H, Wu Y, Dong Y. Forecasting solar radiation using an optimized hybrid model by cuckoo search algorithm. Energy 2015;81(0):627–44.
[22] Aggarwal S, Saini L. Solar energy prediction using linear and non-linear regularization models: a study on {AMS} (american meteorological society) 2013–14 solar energy prediction contest. Energy 2014;78(0):247–56.
[23] Kudo M, Takeuchi A, Nozaki Y, Endo H, Sumita J. Forecasting electric power generation in a photovoltaic power system for an energy network. Electr Eng Jpn 2009;167(4):16–23.
[24] Bacher P, Madsen H, Nielsen HA. Online short-term solar power forecasting. Sol Energy 2009;83(10):1772–83.
[25] M. Hassanzadeh, M. Etezadi-Amoli, M. Fadali, Practical approach for sub-hourly and hourly prediction of pv power output, in: North American Power Symposium (NAPS), 2010, 2010, pp. 1–5.
[26] Lorenz E, Scheidsteger T, Hurka J, Heinemann D, Kurz C. Regional pv power prediction for improved grid integration. Prog Photovolt Res Appl 2011;19(7):757–71.
[27] Nonnenmacher L, Kaur A, Coimbra CFM. Day-ahead resource forecasting for concentrated solar power integration. Renew Energy 2016;86(0):866–76.
[28] Boland J, David M, Lauret P. Short term solar radiation forecasting: island versus continental sites. Energy 2016;113(0):186–92.
[29] Chen C, Duan S, Cai T, Liu B. Online 24-h solar power forecasting based on weather type classification using artificial neural network. Sol Energy 2011;85(11):2856–70.
[30] Shi J, Jen Lee W, Liu Y, Yang Y, Wang P. Forecasting power output of photovoltaic systems based on weather classification and support vector machines. IEEE Trans Ind Appl 2012;48(3):1064–9.
[31] Kaur A, Nonnenmacher L, Pedro HTC, Coimbra CFM. Benefits of solar forecasting for energy imbalance markets. Renew Energy 2016;86(0):819–30.
[32] Yona A, Senjyu T, Funabashi T, Kim C-H. Determination method of insolation prediction with fuzzy and applying neural network for long-term ahead pv power output correction. IEEE Trans Sustain Energy 2013;4(2):527–33.
[33] Yang H, Huang C, Huang Y, Pai Y. A weather-based hybrid method for 1-day ahead hourly forecasting of pv power output. IEEE Trans Sustain Energy 2014;5(3):917–26.

[34] Pedro HTC, Coimbra CFM. Assessment of forecasting techniques for solar power production with no exogenous inputs. Sol Energy 2012;86(7):2017–28.
[35] Larson DP, Pedro HTC, Coimbra CFM. Day-ahead forecasting of solar power output from photovoltaic plants in the American Southwest. Renew Energy 2016;91(0):11–20.
[36] Mejia FA, Kleissl J. Soiling losses for solar photovoltaic systems in California. Sol Energy 2013;95(0):357–63.
[37] Mani M, Pillai R. Impact of dust on solar photovoltaic (pv) performance: research status, challenges and recommendations. Renew Sustain Energy Rev 2010;14(9):3124–31.
[38] Hippert HS, Pedreira CE, Souza RC. Neural networks for short-term load forecasting: a review and evaluation. IEEE Trans Power Syst 2001;16(1):44–55.
[39] Kaur A, Pedro HTC, Coimbra CFM. Ensemble re-forecasting methods for enhanced power load prediction. Energy Convers Manag 2014;80(0):582–90.
[40] Felice MD, Xin Y. Short-term load forecasting with neural network ensembles: a comparative study [application notes]. IEEE Comput Intell Mag 2011;6(3):47–56.
[41] Taylor JW, Buizza R. Using weather ensemble predictions in electricity demand forecasting. Int J Forecast 2003;19(1):57–70.
[42] Chen B-J, Chang M-W, Lin C-J. Load forecasting using support vector machines: a study on eunite competition 2001. IEEE Trans Power Syst 2004;19(4):1821–30.
[43] Quan H, Srinivasan D, Khosravi A. Uncertainty handling using neural network-based prediction intervals for electrical load forecasting. Energy 2014;73(0):916–25.
[44] Ardakani F, Ardehali M. Long-term electrical energy consumption forecasting for developing and developed economies based on different optimized models and historical data types. Energy 2014;65(0):452–61.
[45] Jurado S, Nebot Angela, Mugica F, Avellana N. Hybrid methodologies for electricity load forecasting: entropy-based feature selection with machine learning and soft computing techniques. Energy 2015;86(0):276–91.
[46] Liu N, Tang Q, Zhang J, Fan W, Liu J. A hybrid forecasting model with parameter optimization for short-term load forecasting of micro-grids. Appl Energy 2014;129(0):336–45.
[47] Hong WC. Chaotic particle swarm optimization algorithm in a support vector regression electric load forecasting model. Energy Convers Manag 2009;50(1):105–17.
[48] Kavousi-Fard A, Samet H, Marzbani F. A new hybrid modified firefly algorithm and support vector regression model for accurate short term load forecasting. Expert Syst Appl 2014;41(13):6047–56.
[49] Kaur A, Pedro HTC, Coimbra CFM. Impact of onsite solar generation on system load demand forecast. Energy Convers Manag 2013;75(0):701–9.
[50] Makarov YV, Huang Z, Etingov PV, Ma J, Guttromson RT, Subbarao K, et al. Incorporating wind generation and load forecast uncertainties into power grid operations. no. PNNL-19189. Pacific Northwest National Laboratory; 2010.
[51] Wu J, Botterud A, Mills A, Zhou Z, Hodge B-M, Heaney M. Integrating solar {PV} (photovoltaics) in utility system operations: analytical framework and Arizona case study. Energy 2015;85(0):1–9.
[52] Makrides G, Zinsser B, Norton M, Georghiou GE, Schubert M, Werner JH. Potential of photovoltaic systems in countries with high solar irradiation. Renew Sustain Energy Rev 2010;14(2):754–62.
[53] Stetz T, von Appen J, Niedermeyer F, Scheibner G, Sikora R, Braun M. Twilight of the grids: the impact of distributed solar on Germany's energy transition. Power Energy Mag IEEE 2015;13(2):50–61.
[54] Costa PM, Matos MA, Lopes JAP. Regulation of microgeneration and microgrids. Energy Policy 2008;36(10):3893–904.
[55] Siddiqui A, Marnay C. Distributed generation investment by a microgrid under uncertainty. Energy 2008;33(12):1729–37.
[56] Taha AF, Hachem NA, Panchal JH. A quasi-feed-in-tariff policy formulation in micro-grids: a bi-level multi-period approach. Energy Policy 2014;71:63–75.
[57] Soshinskaya M, Crijns-Graus WHJ, Guerrero JM, Vasquez JC. Microgrids: experiences, barriers and success factors. Renew Sustain Energy Rev 2014;40(0):659–72.
[58] Hyans M, Awai A, Bourgeois T, Cataldo K, Hammer SA, Kelly T, et al. Microgrids: an assessment of the value, opportunities and barriers to deployment in New York state. New York State Energy Research and Development Authority; 2011.
[59] Cortés A, Martínez S. On distributed reactive power and storage control on microgrids. Int J Robust Nonlinear Control 2016;26(14):3150–69.
[60] Cortés A, Martínez S. A hierarchical algorithm for optimal plug-in electric vehicle charging with usage constraints. Automatica 2016;68(0):119–31.
[61] Kuznetsova E, Li Y-F, Ruiz C, Zio E, Ault G, Bell K. Reinforcement learning for microgrid energy management. Energy 2013;59(0):133–46.
[62] Holjevac N, Capuder T, Kuzle I. Adaptive control for evaluation of flexibility benefits in microgrid systems. Energy 2015;92(3):487–504.
[63] Hernández L, Baladrón C, Aguiar JM, Carro B, Sánchez-Esguevillas A, Lloret J. Artificial neural networks for short-term load forecasting in microgrids environment. Energy 2014;75(0):252–64.
[64] T. Bialek, Borrego springs microgrid demonstration project, Prepared for: California Energy Commission CEC-500-2014-067.
[65] M. J. Reno, C. W. Hansen, J. S. Stein, Global horizontal irradiance clear sky models: implementation and analysis, SAND2012-2389, Sandia National Laboratories, Albuquerque, NM.
[66] Ljung L. System identification: theory for the user. ISBN 0-13-881640-9 025. New Jersey, USA: Prentice Hall PTR; 1999.
[67] Vapnik V, Golowich SE, Smola A. Support vector method for function approximation, regression estimation, and signal processing. Adv Neural Inf Process Syst 1997:281–7.
[68] Smola AJ, Scholkopf B. A tutorial on support vector regression. Stat Comput 2004;14(3):199–222.
[69] Lu C-J, Lee T-S, Chiu C-C. Financial time series forecasting using independent component analysis and support vector regression. Decision Support Syst 2009;47(2):115–25.
[70] Fan S, Chen L. Short-term load forecasting based on an adaptive hybrid method. IEEE Trans Power Syst 2006;21(1):392–401.
[71] Huang C-L, Tsai C-Y. A hybrid sofm-svr with a filter-based feature selection for stock market forecasting. Expert Syst Appl 2009;36(2, Part 1):1529–39.
[72] Chang C-C, Lin C-J. LIBSVM: a library for support vector machines. ACM Trans Intell Syst Technol 2011;2:27:1–27:27.
[73] Marquez R, Coimbra CFM. A proposed metric for evaluation of solar forecasting models. J Sol Eng 2012;135(1):0110161–9.
[74] Granger C, Newbold P. Spurious regressions in econometrics. J Econ 1974;2(2):111–20.
[75] Granger C. Some properties of time series data and their use in econometric model specification. J Econ 1981;16(1):121–30.
[76] Granger CWJ. Developments in the study of cointegrated economic variables. Oxf Bull Econ Stat 1986;48(3):213–28.